# Poplar miR472a targeting *NBS-LRRs* is involved in effective defense response to necrotrophic fungus *Cytospora chrysosperma*

Yanyan Su[1], Hui-Guang Li [1], Yonglin Wang[2], Shuang Li[1], Hou-Ling Wang[2], Lu Yu[2], Fang He[1], Yanli Yang[1], Cong-Hua Feng[1], Peng Shuai[1], Chao Liu[1], Weilun Yin[1] and Xinli Xia[1]*

[1]Beijing Advanced Innovation Center for Tree Breeding by Molecular Design, College of Biological Sciences and Technology, National Engineering Laboratory of Tree Breeding, Beijing Forestry University, Beijing 100083, China

[2]College of Forestry, Beijing Forestry University, Beijing 100083, China

Yanyan Su: yanyansu@bjfu.edu.cn

Hui-Guang Li: hg_li@bjfu.edu.cn

Yonglin Wang: yonglinwang@bjfu.edu.cn

Shuang Li: Shuang_LI@bjfu.edu.cn

Hou-Ling Wang: whling@bjfu.edu.cn

Lu Yu: 18304017749@163.com

Fang He: hefang3150174@bjfu.edu.cn

Yan-Li Yang: yangyl@bjfu.edu.cn

Cong-Hua Feng: fengconghua@bjfu.edu.en

Peng Shuai: shuai@fafu.edu.cn

Chao Liu: liuchao1306@163.com

Weilun Yin: yinwl@bjfu.edu.cn

* Corresponding author: Xinli Xia. College of Biological Sciences and Technology, Beijing Forestry University, Beijing 100083, China

E-mail: xiaxl@bjfu.edu.cn

Tel/Fax: 860162336400

**Title：Poplar miR472a targeting *NBS-LRRs* is involved in effective defense response to necrotrophic fungus *Cytospora chrysosperma***

## Highlight

Ptc-miR472a overexpressing poplar exhibited resistance to *Cytospora chrysosperma* and susceptibility to *Colletotrichum gloeosporioides*, while the silenced lines exhibited the opposite phenotype, identifying a new strategy to improve plant disease resistance.

## Abstract

The hemibiotroph *Colletotrichum gloeosporioides* and necrotroph *Cytospora chrysosperma* can cause poplar foliage and stem disease respectively, resulting in substantial economic losses. In this study, *Populus trichocarpa* ptc-miR472a was down-regulated in leaves treated with salicylic acid,

jasmonic acid or bacterial Flagellin (flg22). Here, ptc-miR472a and a short tandem target mimic (STTM) about miR472a were overexpressed respectively in *P. alba* × *P. glandulosa*, and obtained overexpression lines miR472aOE and silenced lines STTM472a. Compared with the STTM472a and WT lines, a lower ROS accumulation was detected both in flg22, *C. gloeosporioides* and *C. chrysosperma* treated miR472aOE plants. In addition, the miR472aOE lines exhibited the highest susceptibility to the hemibiotroph *C. gloeosporioides* but the highest effective defense response to the necrotroph *C. chrysosperma*. JA/ET marker genes *ERF1* was quickly up-regulated in miR472aOE plants. Furthermore, five phasiRNAs (phased, secondary, small interfering RNA) were confirmed in miR472aOE and STTM472a lines, triggering phasiRNAs predicted to enhance the *NBS-LRRs* silencing. Taken together, our study indicated that ptc-miR472a exerts a key role in plant immunity to *C. gloeosporioides* and *C. chrysosperma* by targeting *NBS-LRRs* transcripts. This study provides a new strategy and method for plant breeding to improve plant disease resistance.

**Key words**

MicroRNA, *NBS-LRR*, phasiRNA, *Populus*, *Colletotrichum gloeosporioides,* *Cytospora chrysosperma* ， ROS

## Introduction

Plants inhabit environments thronged with infectious microbes that pose frequent threats to their survival. Accordingly, plants have evolved effective defense systems against the microbes. In this system, R (resistant) proteins

have a pivotal role in response to pathogen infections, and can induce oxidative burst and the expression of pathogenesis-related (*PR*) genes and PCD (programmed cell death) (Jones and Dangl, 2006; Wu *et al.*, 2014; Zou *et al.*, 2018). NBS-LRR proteins that contain a nucleotide-binding site and leucine-rich repeat domains are the largest class of known R proteins. Currently, NBS-LRR proteins have been utilized to defend against biotrophic pathogen-triggered plant diseases by inducing cell death (Zou *et al.*, 2018). HR-associated cell death can confine pathogens by abolishing the nutrient supply, thereby limiting pathogen growth. However, cell death has obviously different roles in plant responses to necrotrophs and biotrophs, as it is an indicator of successful infection by necrotrophs (Mengiste, 2012). For example, plant cell death is beneficial to the necrotrophic pathogen *Botrytis cinerea* and leads to susceptibility (van Kan, 2006). HR and PCD are significantly enriched in the susceptible cultivar sand pear compared to that of the resistant cultivar, and ET and JA levels are highly accumulated in susceptible cultivar (Wang *et al.*, 2017a).

Plant microRNAs (miRNAs) are small noncoding single-stranded RNAs that regulate gene expression at post-transcriptional levels (Axtell, 2013; Zhang *et al.*, 2006a). MiRNAs were reported to play critical roles in regulating growth and development, response to abiotic stress and defense against pathogens (Niu *et al.*, 2016; Weiberg *et al.*, 2014; Xu *et al.*, 2016; Yan *et al.*, 2017). For example, miR156 plays significant roles in development by regulating the expression of *SPL* (SQUAMOSA promoter-binding protein-like) genes that contribute to the juvenile-to-adult vegetative transition and the vegetative-to-reproductive transition (Xu *et al.*, 2016). Additionally, slmiR482f and slmiR5300 are down-regulated in resistant Motelle plants after infection of

tomato by *Fusarium oxysporum* (Ouyang *et al.*, 2014). It has been widely reported that miRNAs could initiate phasiRNAs (phased, secondary small interfering RNAs) produced from noncoding TAS genes and protein-coding genes, such as *NBS-LRRs* (Allen *et al.*, 2005; Fei *et al.*, 2013). Especially in *Arabidopsis*, *M. truncatula* and soybean, miR472 and miR482 could trigger the production of tasiRNAs/phasiRNAs that enhanced the silencing of *NBS-LRR* genes (Boccara *et al.*, 2014; Weiberg *et al.*, 2014; Zhai *et al.*, 2011). It has been reported that miR472a was up-regulated in drought treated *Populus trichocarpa* and *Populus tomentosa* (Ren *et al.*, 2012; Shuai *et al.*, 2013), and down-regulated in salt treated *Populus euphratica* (Li *et al.*, 2013). The Arabidopsis miR472 has been reported to play critical roles in plant immune response by targeting and cleaving *NBS-LRR* transcripts at P-loop-encoding regions (Boccara *et al.*, 2014; Zhai *et al.*, 2011). However, few studies have shown the role of miR472 in the plant immune response to fungal infection, especially in poplars.

*Populus* is an important economic and ecological tree species for its high growth capability and adaptability to the changing environment (Han *et al.*, 2013). *Populus* is widely accepted as model system for wood plants (Narusaka *et al.*, 2012). These plants are also hosts of a large variety of fungi, such as *Colletotrichum gloeosporioides*, *Dothiorella gregaria*, *Melampsora medusae* and *Cytospora chrysosperma* (Miranda *et al.*, 2007; Sun *et al.*, 2016; Wang *et al.*, 2017b). As a hemibiotrophic fungus, *C. gloeosporioides* is highly prevalent in northeast China and results in substantial economic losses, which can cause poplar foliage disease, anthracnose (He *et al.*, 2017; Sun *et al.*, 2016). The necrotrophic fungus *C. chrysosperma* can cause plant stem disease, cankers, which cause serious damage in forest nurseries, young plantations,

and horticultural settings (Jia *et al.*, 2010). However, there are few studies on the immune response mechanism to these two fungi. In this study, we provide for the first time evidence that poplar miR472a protects plants against the necrotrophic fungus *C. chrysosperma* but not the hemibiotrophic fungus *C. gloeosporioides* by targeting *NBS-LRR* transcripts.

## Materials and Methods

### *Plants materials and fungi strains*

*P. alba* × *P. glandulosa* (84K) seedlings were amplified by micropropagation on half-concentrated MS medium supplemented with 0.05mg/L IBA and 0.05 mg/L NAA (Sigma) (He *et al.*, 2018; Leple, 1992). *P. trichocarpa* seedlings were amplified by micropropagation on half-concentrated MS medium. *Arabidopsis* Col-0 was used to overexpress the pro-miR472a: GUS vector (Han *et al.*, 2013).

*C. gloeosporioides* strain BDL-3 and *C. chrysosperma* strain G-YS-11-C1 were provided by Yonglin Wang (ylwang@bjfu.edu.cn). These two fungi were cultured on PDA medium (200 g potato, 20 g glucose, 20 g agar, per litre of water) (Sun *et al.*, 2016).

### *qRT-PCR analysis of mRNAs, miRNAs and phasiRNAs*

Total RNA was extracted from the poplar leaves using the CTAB reagent method described by Ma *et al*. (2010). For mRNAs quantification, first-strand cDNA was synthesized from the total RNA using FastQuant RT Kit (Tiangen, China). QRT-PCR assays were performed using SuperReal PreMix Plus Kit (SYBR Green, Tiangen) with gene-specific primers. Gene-specific primers are listed in Table S4. UBQ was used as an endogenous reference gene (Wang *et al.*, 2014a).

For miRNAs and phasiRNAs quantification, total RNA was extracted as described above, and a poly (A) tail was added to the 3' end of RNA, and reverse transcription was initiated using the miRcute miRNA First-Strand cDNA Synthesis Kit (Tiangen). QRT-PCR assays were performed as previously with conserved forward primer and gene-specific reverse primers.18S was used as an endogenous reference gene. Gene-specific primers used in this analysis are listed in Table S4.

QRT-PCR was performed using an ABI StepOne Plus instrument (Applied Biosystems, Inc., Carlsbad, CA), and the $2^{-\Delta\Delta CT}$ method was used to calculate the relative changes in gene expression based on the qRT-PCR data (Schmittgen and Livak, 2007).

*Promoter analysis*

Following the CTAB method by Wang *et al.* (2016), genomic DNA was extracted from *P. trichocarpa* leaves. Putative promoter regions of ptc-miR472a (1028 bp) was amplified from *P. trichocarpa* genomic DNA and inserted upstream of the *GUS* gene in pCAMBIA1391 vector using *EcoR*I (Fig. S2). The construct was introduced into the *A. tumefaciens* strain EHA105 using the freeze-thaw method for transformation (Wise *et al.*, 2006). Then the *A. tumefaciens* was transformed into *Arabidopsis* Col-0 by the floral dip method (Zhang *et al.*, 2006b). The transgenic lines were selected by their hygromycin resistance. Gene-specific primers used in this analysis are listed in Table S4.

For the analysis of cis-elements in promoter, the putative promoter sequence of ptc-miR472a precursor was analyzed using the PLACE database (http://www.dna.affrc.go.jp/PLACE) (Higo *et al.*, 1999).

*Chemical treatments*

For flg22 treatment, water or 100 nM flg22 (Scilight, Beijing) was injected into the leaves of transformed *Arabidopsis* seedlings. For hormone treatments, SA (5 mM in water), and MeJA (100 mM in 0.1% [v/v] ethanol) were applied as previous reported (Li *et al.*, 2004). MeJA-treated *Arabidopsis* were immediately covered with a transparent lid. Control plants were treated identically with 0.1% (v/v) ethanol in water. Leaves were collected after 4 h of treatment. Each treatment was repeated on four plants.

*Generation of transgenic poplars*

For construction of the miR472a overexpression vector, the pre-miRNA fragment of miR472a (252 bp) was amplified from the genomic DNA and inserted into the plant expression vector PBI121 after the cauliflower mosaic virus *35S* promoter (CaMV35S) sequence using *Bam*HI and *Sac*I. The STTM472a-48 construct was constructed using a method modified from Yan *et al.* (2012). The fragment of STTM472a-48 was synthesized (Sangon) and inserted into the plant expression vector PBI121 after the CaMV35S promoter using *Bam*HI and *Sac*I. These vectors were introduced into the *A. tumefaciens* strain EHA105 as described previously.

For poplar transformation, the *A. tumefaciens* was cultured at 28℃ to $OD_{600}$ = 0.5 in liquid LB medium supplemented with 100 mg/L kanamycin, 50 mg/L rifampicin and 100 μM acetosyringone. Stem internodes of 84k plants (3 mm) were incubated with A. *tumefaciens* for 20 min with slow shaking, and placed on MS medium with 0.05 mg/L TDZ and 0.5 mg/L BA at 24°C in the dark for two weeks, then transferred on selected medium with 50 mg/L Kanamycin in the light (Leple, 1992; Wang *et al.*, 2013; Wang *et al.*, 2011). Wild-type and selected transgenic lines were grown by micropropagation on half-concentrated MS medium supplemented with 0.05mg/L IBA and 0.05 mg/L NAA (Sigma) (He *et al.*, 2018). Gene-specific primers used in this analysis are listed in Table S4.

*Computational prediction of ptc-miR472a Targets*

Target genes of ptc-miR472a in *Populus* were predicted from the *P. trichocarpa*

genome v3.0 by the psRNATarget server (http://plantgrn.noble.org/psRNATarget/) (Dai and Zhao, 2011). The penalty score cutoff of ≤ 4 calculated was applied to potential target sites in the miRNA: mRNA duplexes.

*Degradome data and 5'-rapid amplification of cDNA ends (RACE) validate miR472a targets*

Degradome data (accession number SRP081040) was used to validate the targets (Shuai *et al.*, 2016). Briefly, mRNA cleavage start position was predicted by psRNATarget, if the 5'-end of any RNA degradome fragment overlapped the targets cleavage start position was considered validated.

Total RNA was isolated from a mixture of roots, leaves and stems collected from one-year-old *P. trichocarpa*. A GeneRacer Kit (TaKaRa) was used to process the total RNA and map the 5' terminus of the cleaved transcript as described (Vazquez *et al.*, 2004). The cDNA samples were amplified by nested PCR according to the manufacturer's protocols. Gene-specific primers used in this analysis are listed in Table S4.

*Co-transformation in Nicotiana benthamiana*

For the CaMV35S: NBL1-GUS vector construction, the cDNA fragment of *NBL1* (552 bp) was amplified and inserted upstream of the GUS gene in the plant expression vector pCAMBIA1301 under the control of CaMV*35S* promoter using *Bgl*II. For site-directed mutagenesis, six point mutations in the miRNA binding site of *NBL1* (*NBL1m6*) were designed according to the procedure of Chen (2004) and inserted into the vector pCAMBIA1301 using *Bgl*II. These six point mutations in *NBL1m6* should not change the amino acid sequence, which shown in Figure 2C. The constructs were introduced into the *A. tumefaciens* strain EHA105. Gene-specific primers used in this analysis are listed in Table S4.

*N. benthamiana* seedlings (4–6 weeks old) were used for infiltration as described by Lu *et al*. (2017). The *A. tumefaciens* were cultured to $OD_{600}$= 0.8 in 30 ml liquid LB medium supplemented with 100 mg/L kanamycin, 50 mg/L rifampicin, and diluted to $OD_{600}$ = 0.2 for injection. EHA105-pCAMBIA1301-NBL1/NBL1m6 (NBL1/NBL1m6) and EHA105-PBI 121-ptc-miR472a (miR472a) were mixed in equal volumes, and the mixtures (NBL1+/NBL1m6+) were adjusted to $OD_{600}$ = 0.4, respectively. After injection, the seedlings were incubated at 25℃ for 2 days.

*GUS activity analysis*

Histochemical GUS staining was conducted as previously described (Jefferson *et al.*, 1987). After staining for 24 h, the chlorophyll was cleared off with 75% ethanol (Wang *et al.*, 2013).

GUS activity was measured by monitoring the fluorescence of 4-methylumbelliferone (4-MU) produced by β-glucuronidase substrate 4-methylumbelliferyl β-D-glucuronide (MUG) (Jefferson *et al.*, 1987). Protein concentrations were detected as previously described (Bradford, 1976).

*Pathogenicity assays*

For the *C. gloeosporioides* inoculation, detached leaves of different seedlings were needled, inoculated with 20 µl conidium suspension ($2\times10^6$ conidia/ml) in a humidified chamber and cultured in a 16 h light/ 8 h dark growth chamber at 22 ℃ with 70 µmol $m^{-2}$ $s^{-1}$ light intensity. The lesion area was measured with Adobe Photoshop software at 3 days post inoculation (dpi). Each experiment was performed with at least five replicates.

For the *C. chrysosperma* inoculation, a hole (3 mm) was bored into the detached leaves of different seedlings before inoculation, followed by inoculation with mycelial plugs (4 mm) in a humid chamber and cultured in a 16 h light/ 8 h dark growth chamber at 22 ℃ with 70 µmol $m^{-2}$ $s^{-1}$ light intensity.

For shoot inoculation, 15 cm long of twigs (diameter 0.4 cm-0.8 cm) were washed with tap water, then inoculated with *C. chrysosperma* as described in leaves (Ke *et al.*, 2012). The lesion area was measured with Adobe Photoshop software. Each experiment was performed with at least five replicates.

Leaf cell death was observed by staining with trypan blue solution (10 ml lactic acid, 10 ml glycerol, 10 ml phenol, 40 mg trypan blue, dissolved in 10 ml distilled water) (Fernández-Bautista *et al.*, 2016).

*ROS measurements and callose staining*

The kinetics of flg22-triggered ROS production were assayed using a luminal-based bioassay (Boccara *et al.*, 2014). Leaf discs were incubated in 200 µl $H_2O$ at room temperature overnight, avoiding submersion and shaking. The next morning, 180 µl water and 20 µl luminal master mix (200 µM luminal and 10 µg horseradish peroxidase with or without 1 µM flg22) were added. Luminescence was immediately measured for 45 min using a VARIOSKAN FLASH (Thermo Scientific). At least 25 to 30 discs were tested under these conditions.

DAB (diaminobenzidine) staining was used to measure the accumulation of $H_2O_2$ (Ding *et al.*, 2015). Leaves were immersed in freshly prepared 100 µg/ml DAB solution in the dark for 12 h. Stained leaves were cleared of chlorophyll with 95% ethanol.

The content of $H_2O_2$ in poplar leaves was measured as previous described (Shi *et al.*, 2012). Briefly, 0.5 g leaves were grinded with 50 mM sodium phosphate buffer (pH 7.8), then centrifuged at 12000 rpm for 30 min at 4 ℃. 0.5 ml of the above supernatant was mixed thoroughly with 0.5 ml 0.1% (w/v) titanium sulphate in 20%, v/v $H_2SO_4$) for 10 min.

For callose detection, leaves were infiltrated with 100 nM flg22 or water for 15 h, then cleared, and stained with 0.01% aniline blue (Sigma) for 30 min. Callose deposition was counted with a Leica DM 2500 upright fluorescence microscope (excitation filter 365 nm), and summed using ImageJ software (Li *et al.*, 2010). Each data consisted of at least six replicates.

*Statistical analysis*

The variances of experimental data were analysis using Statistical Product and Service Solutions 17.0 (SPSS). Data were reported as the mean ± standard error (SE). Differences among means for treatments or plant lines were evaluated by Duncan's post hoc test (one-way ANOVA) (Zheng *et al.*, 2013).

## Results

*Analysis of cis-elements in ptc-miR472a promoter sequences*

To analyze the spatial and temporal expression pattern of miR472a, we analyzed the promoter sequence of ptc-miR472a, and found a series of cis-elements (Fig. S1). Most of the cis-elements, such as G-box, I-box and Sp1, respond to light. We also found nine TGAC-containing W-box elements, which have been reported to specifically combine with WRKY proteins (Eulgem *et al.*, 1999). Four MYB binding sites present in many stress-response promoters were also found in this sequence. Two TC repeats related to defense response were marked in this sequence.

*Expression pattern of ptc-miR472a under different conditions*

To investigate the expression profile of miR472a, we detected first the expression level of miR472a by qRT-PCR in *P. trichocarpa* root (R), xylem (X), phloem (P), young leaves (L1), mature leaves (L2), and senescent leaves (L3) under normal growth conditions (Fig. 1A). The results showed that the expression of miR472a was the highest in mature leaves.

The transgenic *Arabidopsis* leaves overexpressing the promoter of miR472a were treated with flagellin-derived peptide (flg22), SA or MeJA. The GUS activity was observed in treated leaves by histochemical staining. Compared to that of the control leaves, reduced GUS activity was observed in the flg22-, SA- and JA- treated leaves (Fig. 1B).

*MiR472a targets NBS-LRR transcripts and triggers phasiRNAs*

To explore the role of miR472a in poplars, nine transgenic poplar lines miR472aOE overexpressing miR472a were obtained. Due to the small size and multiple members of many miRNA families, generating the miRNA genetic mutants by T-DNA insert is not easily applicable to the function study of miRNAs (Wang *et al.*, 2015; Yan *et al.*, 2012). A short tandem target mimic (STTM), designed as shown in the diagram of STTM472a structure (Fig. S3), was applied to trap miR472a (Yan *et al.*, 2012). Nineteen STTM472a transgenic poplar lines were obtained with the trapped miR472a. All transformations were verified by gDNA PCR and cDNA qRT-PCR (Fig. S4).

To identify the target genes of ptc-miR472a in *Populus*, eighty-one candidate genes were predicted using psRNATarget, most of which encode NBS-LRR family proteins (Table S1). Here, we identified that a *NBS-LRR* gene Potri.018G138500 (*NBL1*) was targeted by miR472a using degradome library (Table. S2). *NBL1* was also verified by 5' rapid amplification of cDNA ends (RACE) PCR assay (Fig. 2A). To confirm whether the *NBL1* mRNA was directly cleaved by miR472a, we used a fragment of *NBL1* contains the cleavage site of miR472a, and a mutant of *NBL1* with six mismatches at the cleavage site (*NBL1m6*) for injection (Fig. 2B). After 48 h, we observed the strong staining in NBL1 injected leaves (NBL1), but a lighter staining in leaves that had been co-transformed with miR472a (NBL1+). No significant different staining was observed in the leaves between transformed NBL1m6 (NBL1m6) and co-transformed NBLm6 with miR472a (NBL1m6+) (Fig. 2C). The GUS activity result was consistent with the staining (Fig. 2D). This result

demonstrated that miR472a was in line with a putative direct target *NBL1* transcripts.

Additionally, *NBL1* mRNA showed 50% down-regulation in OE-28 lines and 1.5 times up-regulation in STTM-15 lines (Fig. 3A). *NBL2*, *NBL3* and *NBL4* were described produce phasiRNAs (Shuai *et al.*, 2016), which all exhibited down-regulated and up-regulated expression in miR472aOE and STTM472a lines, respectively.(Fig. 3A). The structure of these four targets were analyzed using SMART (smart.embl-heidelberg.de/) (Fig. 3B).

We also verified the phasiRNAs from these three PHAs which had been predicted in our previous work using qRT-PCR in miR472aOE and STTM472a lines. As a result, five phasiRNAs (SIR14, SIR16, SIR17, SIR21, and SIR25) were up-regulated in miR472aOE lines and down-regulated in STTM472a lines (Fig. 3C). Analyze the targets of these phasiRNAs found that these targets include *NBS-LRR*s and other characterized genes involved in embryonic development, cell differentiation, and $Ca^{2+}$ signalling (Table 1 & S3).

*MiR472a negatively regulated the immunity triggered by flg22 and C. gloeosporioides*

To gain a first insight into the role of miR472a in plant immunity, we infiltrated 84K leaves with 100 nM flg22 to examine the expression level of miR472a in

the flg22-triggered PTI response. A SA marker gene nonexpresser of pathogenesis-related genes 1 (*NPR1*, Potri.012G118300) was up-regulated 1.50 fold compared to that of the not treated control at 30 min, while the miR472a was down-regulated 40% when treated with flg22 for 20 min (Fig. 4A & B). We examined the ROS production in flg22-treated miR472aOE, WT and STTM472a lines using the $H_2O_2$-dependent luminescence reaction. When treated with flg22, a stronger oxidative burst was observed significantly in the WT and STTM472a lines than that in the miR472aOE lines (Fig. 4C). Furthermore, we monitored the formation of cell wall depositions of callose that played a critical role in the basal immunity. No significant difference in $H_2O$ treated leaves was observed among these three lines. When treated with flg22, a significantly different callose deposition was detected among WT, miR472aOE and STTM472a lines (Fig. 4D). The callose deposition in the miR472aOE lines was declined 37% and 67% compared to that of the WT and STTM472a lines, respectively (Fig. 4E). These results indicated that ptc-miR472a negatively regulated the flg22-triggered immune response.

To explore the role of miR472a in plant defense against the hemibiotrophic fungus *C. gloeosporioides*, the detached leaves of WT, miR472aOE and STTM472a lines were inoculated with *C. gloeosporioides*. At 3 dpi, the trypan blue staining of these three different lines indicated that the virulence of *C. gloeosporioides* appeared in miR472aOE leaves was two- and eleven- fold higher than that in the WT and STTM472a lines, respectively (Fig. 5A-C). These data indicated that overexpression of miR472a rendered the plant susceptible to *C. gloeosporioides*. We detected the accumulation of $H_2O_2$ in leaves of WT, miR472aOE and STTM472a lines by DAB staining at 0 and 24 hpi. Compared with that in the WT and STTM472a lines, a lower ROS

accumulation was detected both in the control and in the inoculated leaves of miR472aOE plants (Fig. 5D-F). To understand the expression profile of miR472a in inoculated leaves, we sampled the WT leaves at different inoculation times and measured the expression level of miR472a by qRT-PCR. The data indicated that miR472a was down-regulated and declined 70% at 72 hpi (Fig. 5G). We also detected the target genes *NBL1-NBL4* in these samples, and the expression of these targets transcripts was up-regulated approximately three fold compared to that of the control (Fig. 5H).

*Ptc-miR472a-overexpressing plants exhibited enhanced resistance to necrotrophic pathogen C. chrysosperma*

To determined how the miR472a acts in the necrotrophic pathogen infection, the detached leaves from WT, miR472aOE and STTM472a lines were inoculated with *C. chrysosperma*. The trypan blue staining of these three different lines indicated that the lowest virulence was observed in miR472aOE leaves at 2 dpi (Fig. 6A & B). The lesion size of miR472aOE lines was 28% less than that of the WT lines and 54% less than that of the STTM472a lines (Fig. 6D). We also compared the ROS accumulation in these three inoculated leaves, and a lower $H_2O_2$ accumulation around the inoculation site was detected in the miR472aOE lines (Fig. 6C). Stems from 3-month-old miR472aOE, WT and STTM472a lines were also inoculated with *C. chrysosperma*. At 6 dpi, the virulence of *C. chrysosperma* appeared on all stems, and STTM472a lines had the largest lesion (Fig. 6E). We also inoculated the 8-month-old stems from WT and miR472aOE plants, the OE-13

and OE-35 lines exhibited 15% and 42% smaller lesions than those of the WT, respectively (Fig. 6F & G).

To test whether JA/ET signalling involved in the response to *C. chrysosperma*, we measured the expression level of MeJA/ET-related marker genes *ERF1* (ethylene response factor 1, Potri.005G223200.1) in inoculated WT, miR472aOE and STTM472a lines. The results showed that *ERF1* exhibited significant higher expression level in the miR472aOE lines at 2 dpi, and lower expression level after 2 dpi than those in the WT and STTM472a lines (Fig. 7C & D). We also measured the expression level of *PR3* (Potri.004G182000.1), *MPK3* (Potri.001G271700.1) and *MPK6* (Potri.007G139800.1), *PR3* exhibited the highest expression at 2 dpi, 6 dpi and 8 dpi in miR472aOE, WT and STTM472a lines, respectively, while the *MPK3* exhibited the highest expression at 4 dpi in miR472aOE lines, and at 8 dpi in WT and STTM472a lines, *MPK6* did not exhibited the similar expression trend to *MPK3* until 8 dpi (Fig. 7).

## Discussion

As an effective approach for decreasing the expression of miRNAs, STTM has been used in many plants, such as *Arabidopsis*, tobacco (*Nicotiana tabacum*), rice (*Oryza sativa*) and soybean (*Glycine max*) (Wang *et al.*, 2014b; Yan *et al.*, 2012; Yan *et al.*, 2016). In this study, STTM was highly effective and specific in reducing the level of miR472a in poplar (Fig. S4C & D).

In early studies, miR472 was considered to be a member of miR482/miR2118 family, which targets the NBS-LRR family at P-Loop (Shivaprasad *et al.*, 2012), and triggers the production of tasiRNAs/phasiRNAs in *Arabidopsis* (Boccara, Sarazin et al. 2014). In this study, we domonstrated that *NBL1* mRNA was targeted by miR472a using four methods which included degradome libraries of *P. trichocarpa,* 5' RACE, co-transformation in *N. benthamiana* and qRT-PCR in miR472aOE and STTM472a lines (Fig. 2 & 3A). We also found three other targets with opposite transcriptional expression levels in overexpressed and knock-down miR472a poplar lines (Fig. 3A).

In our previous study, we have identified 12 phasiRNAs induced by miR472a from four PHA genes by Illumina sequencing in *P. trichocarpa* (Shuai *et al.*, 2016). In this study, we verified five phasiRNAs that were triggered by miR472a in three PHAs (Fig. 3C, Fig. S5). Analyze the locations of these phasiRNAs in PHA genes demonstrated that they all clustered downstream of the cleavage site in PHAs (Fig. S6). These phasiRNAs are predicted to target and down-regulate other *NBS-LRR* genes (Table 1 & S2). For example, SIR16 was predicted to target *NBS-LRRs* (Potri.005G008700.1, Potri.005G009100.1 and Potri.005G009400.1), SIR21 and SIR25, which came from *NBL4*, were predicted to target *NBL2*. These predictions suggest that the expression of *NBS-LRR* genes was strictly controlled by miR472a in *populus*. This result was consistent with previous reports that miR472 can be a master regulator and play a significant role in modulating the abundance of many *NBS-LRR* transcripts (Weiberg *et al.*, 2014; Zhai *et al.*, 2011; Zhang *et al.*, 2016). Based on these results, we propose a model, which integrates the contribution of the miR472a-dependent PTGS (post-transcriptional gene silencing) pathway in plant immunity (Fig. 8). Under unchallenged conditions, miR472a is

constitutively expressed and down-regulate a subset of *NBS-LRR* mRNAs at the post-transcriptional level (Fig. 8A).

SA is a systemic signal for plant resistance against many biotrophs, whereas JA was described to promote the defense against necrotrophs (Jones and Dangl, 2006). In this study, a series of stress response cis-elements were predicted in the promoter of ptc-miR472a (Fig. S1), stronger GUS staining was observed in control *Arabidopsis* leaves and lower GUS staining in SA and MeJA treated leaves, which indicated that miR472a is continuously expressed in normal condition and was down-regulated when plants responded to pathogens (Fig. 1B). This finding verified the hypothesis that miRNAs maintain the expression of NBS-LRR at a low level under normal conditions, but up-regulated R proteins and triggered a defense response when plants suffered attacks from pathogens (Weiberg *et al.*, 2014). Recent evidence suggests that flg22 triggers the PTI causing leaves to produce ROS quickly and deposit callose (Boccara *et al.*, 2014; Weiberg *et al.*, 2014). In this study, the lower GUS staining and down-regulated miR472a expression level were detected in flg22-treated *Arabidopsis* and poplar leaves (Fig. 1B & 4B), which indicted that miR472a was down-regulated when the plant suffered the PAMP (pathogen associated molecular pattern), such as flg22. In addition, when treated with flg22, the miR472aOE lines has the lowest oxidative burst and callose deposition compared to WT and STTM472a lines (Fig. 4C-E), which indicated that miR472a negatively regulated flg22-triggered immune response.

Hemibiotrophs display an early biotrophic phase followed by the necrotrophic mode of nutrition (Mengiste, 2012). In this study, the greater lesion size and

cell death appeared in *C. gloeosporioides*-treated miR472aOE leaves but less in the other two lines, especially in the STTM472a lines (Fig. 5A-C). The transcription level of miR472a was also down-regulated in *C. gloeosporioides* treated leaves (Fig. 5G), which indicated that miR472a negatively regulated the immunity triggered by *C. gloeosporioides*. The target genes of miR472a, *NBL1-NBL4*, were up-regulated in *C. gloeosporioides*-treated leaves (Fig. 5H), which indicated that these four NBS-LRRs were involved in the defense against *C. gloeosporioides.* In addition, plant-produced ROS are crucial for resistance against hemibiotrophs mainly by regulating cell death (Mengiste, 2012). The lower ROS accumulation was observed in miR472aOE lines both in the control and inoculated leaves (Fig. 5D-F). We thus propose that upon pathogen detection, miR472a is down-regulated and in concert with the enhanced accumulation of NBS-LRR mRNAs/ proteins, the enhanced NBS-LRRs promote the immune response including the production of ROS and HR to defense against *C. gloeosporioides* (Fig. 8B).

Although ROS is crucial for resistance to hemibiotrophs, some observations suggest that ROS benefit the necrotrophs by leading to cell death (Mengiste, 2012). The higher level of ET, HR and PCD were described in susceptible cultivar compared to resistant cultivar (Wang *et al.*, 2017a). Many necrotrophs secrete toxins, CWDEs, NEPs, oxalic acid, that serve as virulence factors and result in immune response and necrosis (Oliver and Solomon, 2010). The NB-ARC domain of plant R proteins was described to induce cell death (van Ooijen *et al.*, 2008). In this study, these four target genes *NBL1-NBL4* all had a NB-ARC domain in their proteins, which probably benefit the PCD (Fig. 3B). When WT, miR472aOE and STTM472a lines were inoculated with *C. chrysosperma*, the STTM472a lines exhibited the largest lesion, and their

leaves exhibited the highest ROS accumulation (Fig. 6A-D), indicating that excessive R proteins amounts may cause an extreme immune response including PCD and ROS burst, resulting in necrosis and susceptibility (Fig. 8C).

JA plays a key role in plant response against necrotrophic pathogens by inducing the production of secondary metabolites (Li *et al.*, 2018). JA/ET signal marker gene *ERF1* is a positive regulator of resistance to necrotrophs, overexpressing of *ERF1* in Arabidopsis confers resistance to necrotrophic fungi *Botrytis cinerea* (Berrocal-Lobo *et al.*, 2002; Mengiste, 2012). In this study, *ERF1* exhibited the significant highest expression level at 2 dpi in miR472aOE lines (Fig. 7B), this indicated that miR472aOE lines may be more sensitive to *C. chrysosperma*, and promote the JA/ET signal to quickly response to this fungus. Basic chitinase *PR3* causes fungal cell wall chitin hydrolysis (Liu *et al.*, 2016). *MPK3/MPK6* contribute positively to the immunity response by ROS accumulation and HR, as well as ET accumulation (Su *et al.*, 2018). In this study, the highest expression level of *PR3* and *MPK3* in STTM472a lines may indicate the highest numbers of *C. chrysosperma* in this lines (Fig 7A & D). *MPK6* did not exhibited the similar expression trend to *MPK3* until 8 dpi, which might indicate the different role of *MPK6* in *C. chrysosperma* treated poplars. Prolonged activation of *MPK3* and *MPK6* result in the inhibition of photosynthesis and accumulation of ROS in the chloroplasts when plants exposed to pathogens (Su *et al.*, 2018). In this study, whether *MPK3* effected the photosynthesis during *C. chrysosperma* triggered immunity need to be verified in further researches.

## Additional files

Fig. S1. Analysis of cis-elements from the promoter sequence of miR472a.

Fig. S2. Diagram of pro-miR472a: GUS structure.

Fig. S3. Diagram of STTM472a-48 structure.

Fig. S4. Confirmation of ptc-miR472a overexpression and silenced plants.

Fig. S5. The location of phasiRNAs in the PHAs.

Table S1. Results of predicted targets of miR472a.

Table S2 Degradome data validate the *NBL1* transcript targeted by miR472a.

Table S3. Results of predicted targets of phasiRNAs.

Table S4. List of primers used in this study.

## Acknowledgments

This study was supported by the State '13.5' Key Research Programme of China (No. 2016YFD0600102) and the project of the National Natural Science Foundation of China (31570308, 31600484, 31770649). The authors declare no conflict of interest.

## Reference

**Allen E, Xie Z, Gustafson AM, Carrington JC**. 2005. microRNA-directed phasing during trans-acting siRNA biogenesis in plants. Cell **121**, 207-221.

**Axtell MJ**. 2013. Classification and comparison of small RNAs from plants. Annual Review of Plant Biology **64**, 137-159.

**Berrocal-Lobo M, Molina A, Solano R**. 2002. Constitutive expression of ETHYLENE-RESPONSE-FACTOR1inArabidopsisconfers resistance to several necrotrophic fungi. The Plant Journal **29**, 23-32.

**Boccara M, Sarazin A, Thiebeauld O, Jay F, Voinnet O, Navarro L, Colot V**. 2014. The Arabidopsis miR472-RDR6 silencing pathway modulates PAMP- and effector-triggered immunity through the post-transcriptional control of disease resistance genes. PLoS Pathogens **10**, e1003883.

**Bradford MM**. 1976. A rapid and sensitive method for the quantitation of microgram quantities of protein utilizing the principle of protein-dye binding. Analytical Biochemistry **72**, 248-254.

**Chen X**. 2004. A MicroRNA as a Translational Repressor of APETALA2 in Arabidopsis Flower Development. Science **303**, 2022-2025.

**Dai X, Zhao PX**. 2011. psRNATarget: a plant small RNA target analysis server. Nucleic Acids Research **39**, 155-159.

**Ding S, Zhang B, Qin F**. 2015. Arabidopsis RZFP34/CHYR1, a Ubiquitin E3 Ligase, Regulates Stomatal Movement and Drought Tolerance via SnRK2.6-Mediated Phosphorylation. The Plant Cell **27**, 3228-3244.

**Eulgem T, Rushton PJ, Schmelzer E, Hahlbrock K, Somssich IE**. 1999. Early nuclear events in plant defence signalling: rapid gene activation by WRKY transcription factors. The EMBO Journal **18**, 4689-4699.

**Fei Q, Xia R, Meyers BC**. 2013. Phased, secondary, small interfering RNAs in posttranscriptional regulatory networks. The Plant Cell **25**, 2400-2415.

**Fernández-Bautista N, Domínguez-Núñez J, Moreno MM, Berrocal-Lobo M**. 2016. Plant Tissue Trypan Blue Staining During Phytopathogen Infection. Bio-Protocol **6**, e2078.

**Han X, Tang S, An Y, Zheng DC, Xia XL, Yin WL**. 2013. Overexpression of the poplar NF-YB7 transcription factor confers drought tolerance and improves water-use efficiency in Arabidopsis. Journal of Experimental Botany **64**, 4589-4601.

**He F, Wang HL, Li HG, Su Y, Li S, Yang Y, Feng CH, Yin W, Xia X**. 2018. PeCHYR1, a ubiquitin E3 ligase from Populus euphratica, enhances drought tolerance via ABA-induced stomatal closure by ROS production in Populus. Plant Biotechnology Journal **16**, 1514-1528.

**He P, Wang Y, Wang X, Zhang X, Tian C**. 2017. The Mitogen-Activated Protein Kinase CgMK1 Governs Appressorium Formation, Melanin Synthesis, and Plant Infection of Colletotrichum gloeosporioides. Frontiers in Microbiology **8**, 2216.

**Higo K, Ugawa Y, Iwamoto M, Korenaga T**. 1999. Plant cis-acting regulatory DNA elements (PLACE) database: 1999. Nucleic Acids Research **27**, 297-300.

**Jefferson RA, Kavanagh TA, Bevan MW**. 1987. GUS fusions: beta-glucuronidase as a sensitive and versatile gene fusion marker in higher plants. The EMBO Journal **6**, 3901-3907.

**Jia Z, Sun Y, Yuan L, Tian Q, Luo K**. 2010. The chitinase gene (Bbchit1) from Beauveria bassiana enhances resistance to Cytospora chrysosperma in Populus tomentosa Carr. Biotechnology Letters **32**, 1325-1332.

**Jones JD, Dangl JL**. 2006. The plant immune system. Nature **444**, 323-329.

**Ke X, Huang L, Han Q, Gao X, Kang Z**. 2012. Histological and cytological investigations of the infection and colonization of apple bark by Valsa mali var. mali. Australasian Plant Pathology **42**, 85-93.

**Leple JC, Brasileiro, A.C.M., Michel, M.F. et al.** 1992. Transgenic poplars: expression of chimeric genes using four different constructs. Plant Cell Reports **11**, 137.

**Li B, Duan H, Li J, Deng XW, Yin W, Xia X**. 2013. Global identification of miRNAs and targets in Populus euphratica under salt stress. Plant Molecular Biology **81**, 525-539.

**Li J, Brader G, Palva ET**. 2004. The WRKY70 transcription factor: a node of convergence for jasmonate-mediated and salicylate-mediated signals in plant defense. The Plant Cell **16**, 319-331.

**Li J, Zhang K, Meng Y, Hu J, Ding M, Bian J, Yan M, Han J, Zhou M**. 2018. Jasmonic acid/ethylene signaling coordinates hydroxycinnamic acid amides biosynthesis through ORA59 transcription factor. The Plant Journal **95**, 444-457.

**Li Y, Zhang Q, Zhang J, Wu L, Qi Y, Zhou JM**. 2010. Identification of microRNAs involved in pathogen-associated molecular pattern-triggered plant innate immunity. Plant Physiology **152**, 2222-2231.

**Liu H, Carvalhais LC, Kazan K, Schenk PM**. 2016. Development of marker genes for jasmonic acid signaling in shoots and roots of wheat. Plant Signaling & Behavior **11**, e1176654.

**Lu X, Dun H, Lian C, Zhang X, Yin W, Xia X**. 2017. The role of peu-miR164 and its target PeNAC genes in response to abiotic stress in Populus euphratica. Plant Physiology and Biochemistry **115**, 418-438.

**Ma HS, Liang D, Shuai P, Xia XL, Yin WL**. 2010. The salt- and drought-inducible poplar GRAS protein SCL7 confers salt and drought tolerance in Arabidopsis thaliana. Journal of Experimental Botany **61**, 4011-4019.

**Mengiste T**. 2012. Plant immunity to necrotrophs. Annual Review of Phytopathology **50**, 267-294.

**Miranda M, Ralph SG, Mellway R, White R, Heath MC, Bohlmann J, Constabel CP**. 2007. The transcriptional response of hybrid poplar (Populus trichocarpa x P. deltoides) to infection by Melampsora medusae leaf rust involves induction of flavonoid pathway genes leading to the accumulation of proanthocyanidins. Molecular Plant-Microbe Interactions **20**, 816-831.

**Narusaka M, Ohtani M, Demura T, Shimada R, Shirasu K, Narusaka Y**. 2012. Development of a model system comprising Populus as a model tree and Colletotrichum gloeosporioides as a model pathogen for studying host-pathogen interactions. Plant Biotechnology **29**, 511-514.

**Niu D, Lii YE, Chellappan P, Lei L, Peralta K, Jiang C, Guo J, Coaker G, Jin H**. 2016. miRNA863-3p sequentially targets negative immune regulator ARLPKs and positive regulator SERRATE upon bacterial infection. Nature Communications **7**, 11324.

**Oliver RP, Solomon PS**. 2010. New developments in pathogenicity and virulence of necrotrophs. Current Opinion in Plant Biology **13**, 415-419.

**Ouyang S, Park G, Atamian HS, Han CS, Stajich JE, Kaloshian I, Borkovich KA**. 2014. MicroRNAs suppress NB domain genes in tomato that confer resistance to Fusarium oxysporum. PLoS Pathogens **10**, e1004464.

**Ren Y, Chen L, Zhang Y, Kang X, Zhang Z, Wang Y**. 2012. Identification of novel and conserved Populus tomentosa microRNA as components of a response to water stress. Functional & Integrative Genomics **12**, 327-339.

**Schmittgen TD, Livak KJ**. 2007. Analyzing real-time PCR data by the comparative C(T) method. Nature Protocols **3**, 1101-1108.

**Shi H, Wang Y, Cheng Z, Ye T, Chan Z**. 2012. Analysis of natural variation in bermudagrass (Cynodon dactylon) reveals physiological responses underlying drought tolerance. PloS One **7**, e53422.

**Shivaprasad PV, Chen HM, Patel K, Bond DM, Santos BA, Baulcombe DC**. 2012. A microRNA superfamily regulates nucleotide binding site-leucine-rich repeats and other mRNAs. The Plant Cell **24**, 859-874.

**Shuai P, Liang D, Zhang Z, Yin W, Xia X**. 2013. Identification of drought-responsive and novel Populus trichocarpa microRNAs by high-throughput sequencing and their targets using degradome analysis. BMC Genomics **14**, 233.

**Shuai P, Su Y, Liang D, Zhang Z, Xia X, Yin W**. 2016. Identification of phasiRNAs and their drought- responsiveness in Populus trichocarpa. FEBS Letters **590**, 3616-3627.

**Su J, Yang L, Zhu Q, Wu H, He Y, Liu Y, Xu J, Jiang D, Zhang S**. 2018. Active photosynthetic inhibition mediated by MPK3/MPK6 is critical to effector-triggered immunity. PLoS Biology **16**, e2004122.

**Sun Y, Wang Y, Tian C**. 2016. bZIP transcription factor CgAP1 is essential for oxidative stress tolerance and full virulence of the poplar anthracnose fungus Colletotrichum gloeosporioides. Fungal Genetics and Biology **95**, 58-66.

**van Kan JA**. 2006. Licensed to kill: the lifestyle of a necrotrophic plant pathogen. Trends in Plant Science **11**, 247-253.

**van Ooijen G, Mayr G, Kasiem MM, Albrecht M, Cornelissen BJ, Takken FL**. 2008. Structure-function analysis of the NB-ARC domain of plant disease resistance proteins. Journal of Experimental Botany **59**, 1383-1397.

**Vazquez F, Vaucheret H, Rajagopalan R, Lepers C, Gasciolli V, Mallory AC, Hilbert JL, Bartel DP, Crete P**. 2004. Endogenous trans-acting siRNAs regulate the accumulation of Arabidopsis mRNAs. Molecular Cell **16**, 69-79.

**Wang C, Bao Y, Wang Q, Zhang H**. 2013. Introduction of the rice CYP714D1 gene into Populus inhibits expression of its homologous genes and promotes growth, biomass production and xylem fibre length in transgenic trees. Journal of Experimental Botany **64**, 2847-2857.

**Wang C, Liu S, Dong Y, Zhao Y, Geng A, Xia X, Yin W**. 2016. PdEPF1 regulates water-use efficiency and drought tolerance by modulating stomatal density in poplar. Plant Biotechnology Journal **14**, 849-860.

**Wang H, Lin J, Chang Y, Jiang CZ**. 2017a. Comparative Transcriptomic Analysis Reveals That Ethylene/H2O2-Mediated Hypersensitive Response and Programmed Cell Death Determine the Compatible Interaction of Sand Pear and Alternaria alternata. Frontiers in Plant Science **8**, 195.

**Wang H, Wang C, Liu H, Tang R, Zhang H**. 2011. An efficient Agrobacterium-mediated transformation and regeneration system for leaf explants of two elite aspen hybrid clones Populus alba x P. berolinensis and Populus davidiana x P. bolleana. Plant Cell Reports **30**, 2037-2044.

**Wang HL, Chen J, Tian Q, Wang S, Xia X, Yin W**. 2014a. Identification and validation of reference genes for Populus euphratica gene expression analysis during abiotic stresses by quantitative real-time PCR. Physiologia Plantarum **152**, 529-545.

**Wang L, Ran L, Hou Y, Tian Q, Li C, Liu R, Fan D, Luo K**. 2017b. The transcription factor MYB115 contributes to the regulation of proanthocyanidin biosynthesis and enhances fungal resistance in poplar. New Phytologist **215**, 351-367.

**Wang Y, Li K, Chen L, Zou Y, Liu H, Tian Y, Li D, Wang R, Zhao F, Ferguson BJ, Gresshoff PM, Li X**. 2015. MicroRNA167-Directed Regulation of the Auxin Response Factors GmARF8a and GmARF8b Is Required for Soybean Nodulation and Lateral Root Development. Plant Physiology **168**, 984-999.

**Wang Y, Wang L, Zou Y, Chen L, Cai Z, Zhang S, Zhao F, Tian Y, Jiang Q, Ferguson BJ, Gresshoff PM, Li X**. 2014b. Soybean miR172c targets the repressive AP2 transcription factor NNC1 to activate ENOD40 expression and regulate nodule initiation. The Plant Cell **26**, 4782-4801.

**Weiberg A, Wang M, Bellinger M, Jin H**. 2014. Small RNAs: a new paradigm in plant-microbe interactions. Annual Review of Phytopathology **52**, 495-516.

**Wise AA, Liu Z, Binns AN**. 2006. Three Methods for the Introduction of Foreign DNA into Agrobacterium. Methods in Molecular Biology **343**, 43.

**Wu L, Chen H, Curtis C, Fu ZQ**. 2014. Go in for the kill: How plants deploy effector-triggered immunity to combat pathogens. [Corrected]. Virulence **5**, 710-721.

**Xu M, Hu T, Zhao J, Park MY, Earley KW, Wu G, Yang L, Poethig RS**. 2016. Developmental Functions of miR156-Regulated SQUAMOSA PROMOTER BINDING PROTEIN-LIKE (SPL) Genes in Arabidopsis thaliana. PLoS Genetics **12**, e1006263.

**Yan J, Gu Y, Jia X, Kang W, Pan S, Tang X, Chen X, Tang G**. 2012. Effective small RNA destruction by the expression of a short tandem target mimic in Arabidopsis. The Plant Cell **24**, 415-427.

**Yan J, Wang P, Wang B, Hsu CC, Tang K, Zhang H, Hou YJ, Zhao Y, Wang Q, Zhao C, Zhu X, Tao WA, Li J, Zhu JK**. 2017. The SnRK2 kinases modulate miRNA accumulation in Arabidopsis. PLoS Genetics **13**, e1006753.

**Yan J, Zhao C, Zhou J, Yang Y, Wang P, Zhu X, Tang G, Bressan RA, Zhu JK**. 2016. The miR165/166 Mediated Regulatory Module Plays Critical Roles in ABA Homeostasis and Response in Arabidopsis thaliana. PLoS Genetics **12**, e1006416.

**Zhai J, Jeong DH, De Paoli E, Park S, Rosen BD, Li Y, Gonzalez AJ, Yan Z, Kitto SL, Grusak MA, Jackson SA, Stacey G, Cook DR, Green PJ,**

**Sherrier DJ, Meyers BC**. 2011. MicroRNAs as master regulators of the plant NB-LRR defense gene family via the production of phased, trans-acting siRNAs. Genes & Development **25**, 2540-2553.

**Zhang B, Pan X, Cobb GP, Anderson TA**. 2006a. Plant microRNA: a small regulatory molecule with big impact. Developmental Biology **289**, 3-16.

**Zhang X, Henriques R, Lin SS, Niu QW, Chua NH**. 2006b. Agrobacterium-mediated transformation of Arabidopsis thaliana using the floral dip method. Nature Protocols **1**, 641-646.

**Zhang Y, Xia R, Kuang H, Meyers BC**. 2016. The Diversification of Plant NBS-LRR Defense Genes Directs the Evolution of MicroRNAs That Target Them. Molecular Biology and Evolution **33**, 2692-2705.

**Zheng D, Han X, An YI, Guo H, Xia X, Yin W**. 2013. The nitrate transporter NRT2.1 functions in the ethylene response to nitrate deficiency in Arabidopsis. Plant, Cell & Environment **36**, 1328-1337.

**Zou S, Wang H, Li Y, Kong Z, Tang D**. 2018. The NB-LRR gene Pm60 confers powdery mildew resistance in wheat. New Phytologist **218**, 298-309.

Table 1. Description of phasiRNAs and the number of targeted transcripts.

| PHAs | PhasiRNAs | Sequence | Number of target transcripts (Expectation ≤ 4) |
|---|---|---|---|
| Potri.008G220200 (*NBL2*, PHA5) | SIR14 | TCTTCTCATAGACAGCTCTAG | 43 |
| Potri.018G137900 (*NBL3*, PHA4) | SIR16 | AACATGTTTATTGGGTGATCG | 63 |
| Potri.018G137900 (*NBL3*, PHA4) | SIR17 | TTAAACCTATACGTCTTGCGA | 32 |
| Potri.T046000 (*NBL4*, PHA3) | SIR21 | TGCTAAAATCGCGAGACACAA | 33 |
| Potri.T046000 (*NBL4*, PHA3) | SIR25 | TACTGTGCTGCAATCTTTTAA | 48 |

**Figure legends:**

Fig. 1. Expression pattern of ptc-miR472a. (A) Relative expression level of ptc-miR472a in young leaves (L1), mature leaves (L2), senescent leaves (L3), phloem (P), xylem (X), and roots (R) of *P. trichocarpa*. (B) The staining of *Arabidopsis* leaves that contain pro-miR472a: GUS treated with $H_2O$, flg22, 0.1% (v/v) ethanol, MeJA, or SA. Bar = 5 mm.

Fig. 2. Experimental validation of targets of miR472a. (A) The cleavage sites of *NBL1* were determined by the modified 5′ RNA ligase-mediated RACE. *NBL1* sequence from 5′ to 3′ and ptc-miR472a sequence from 3′ to 5′ are shown. Watson–Crick pairing (vertical dashes) and G: U wobble pairing (circles) are indicated. Vertical arrows indicate the 5′ termini of miRNA-guided cleavage products, as identified by 5′ RACE, with the frequency of clones shown. (B) Diagram of NBL1 and NBL1m6 structures showed the design strategy with the same amino acid sequence. Histochemical staining (C) and 4-MU production (D) displayed the expression of different transformation (either NBL1/NBL1m6 individually or co-transformed with 35S:miR472a) in *N. benthamiana* leaves (NBL1+ and NBL1m6+ indicated co-transformed NBL1 or NBL1m6 with miR472a). Bar = 1 cm.

Fig. 3. MiR472a targets *NBL1-NBL4* mRNAs and triggers phasiRNAs. The relative expression level of four positive targets *NBL1* to *NBL4* (A) and five

phasiRNAs triggered by miR472a (C) in WT, miR472aOE and STTM472a lines. (B) The predicted structure of targets (*NBL1* to *NBL4*).

Fig. 4. MiR472a negatively regulated the immunity in plants treated with flg22. Relative expression levels of miR472a (A) and *NPR1* (B) detected by RT-qPCR in 84k leaves treated with 100 nM flg22. (C) $H_2O_2$-dependent luminesecence indicated ROS production upon treated of WT, miR472aOE and STTM472a leaf discs with $H_2O$ or flg22 (1 mM). (D & E) Callose deposition upon treatment of WT, miR472aOE and STTM472a leaves with $H_2O$ or flg22 (100 nM). UBQ and 18S were used as endogenous reference genes for *NPR1* and miR472a data normalization, respectively. Different letters indicate significant differences at $P \leq 0.05$ (one-way ANOVA). Bar = 200 μm.

Fig. 5. MiR472a negatively regulated the immunity in response to *C. gloeosporioides*. (A & C) The virulence of *C. gloeosporioides* in WT, miR472aOE and STTM472a leaves. (B) Trypan blue staining demonstrated the virulence of *C. gloeosporioides*. ROS production measured by DAB staining at 0 h (D) and 24 hpi (E). Bar=1 cm. (F) Quantitative measurement of $H_2O_2$ content at 0 and 24 hpi. Transcriptional expression levels of miR472a (G) and its target genes (H) detected by qRT-PCR in 84k leaves treated with *C. gloeosporioides*. UBQ and 18S were used as endogenous reference genes for targets and miR472a data normalization, respectively. Different letters indicate significant differences at $P \leq 0.05$ (one-way ANOVA).

Fig. 6. MiR472a conferred resistance to *C. chrysosperma*. (A & D) The virulence of *C. chrysosperma* in leaves of WT, miR472aOE and STTM472a plants. (B) Trypan blue staining demonstrated the virulence of *C. chrysosperma*. (C) DAB staining in WT, miR472aOE and STTM472a leaves treated with *C. chrysosperma* at 24 hpi. The virulence of *C. chrysosperma* in 3-month-old stems of WT, miR472aOE and STTM472a plants (E) and in 8-month-old stems of WT and miR472aOE plants (F & G). Bar = 1 cm.

Fig. 7. The relative expression levels of *ERF1*, *PR3*, *MPK3* and *MPK6* in *C. chrysosperma* treated different lines. UBQ were used as endogenous reference genes. Different letters indicate significant differences at $P \leq 0.05$ (one-way ANOVA).

Fig. 8. The pathway by which miR472 regulates the plant immunity. (A) Under normal growth condition, miR472a controls the NBS-LRRs at a low level via post-transcriptional gene silencing. (B) When the plants are exposed to hemibiotrophic fungus *C. gloeosporioides*, miR472a is down-regulated and *NB-LRRs* are up-regulated, leading to ROS burst and HR response in plant cells. ROS and HR response counteract the *C. gloeosporioides* infection. (C) When the plants are exposed to necrotrophic pathogen *C. chrysosperma*, R proteins act as a negative regulator to cause plant cell necrosis, and result in susceptibility. *MPK3* induces the JA/ET signalling pathways and immune response. Bold lines indicate increased pathways, while thin lines indicate decreased pathways.

**Figure 1**

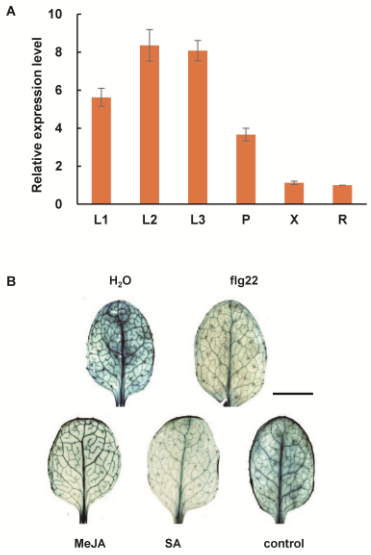

**Figure 2**

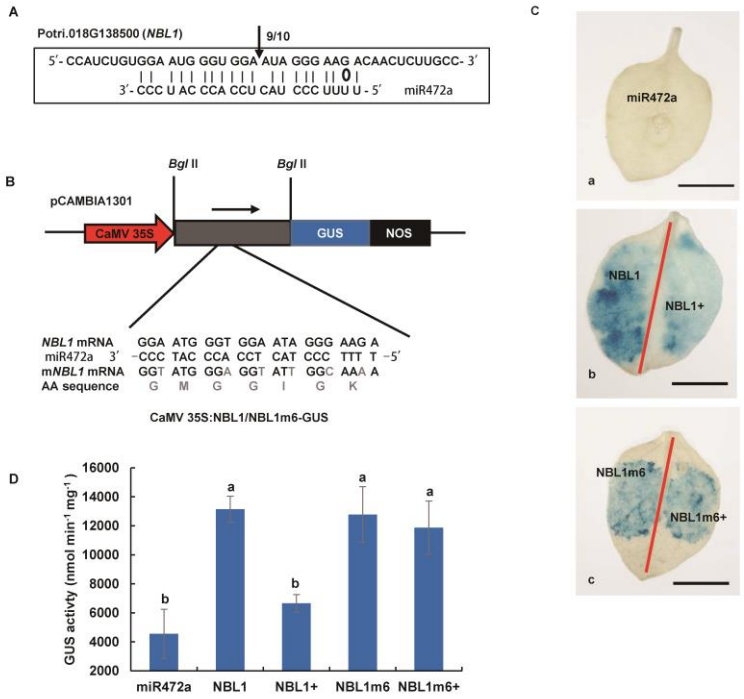

**Figure 3**

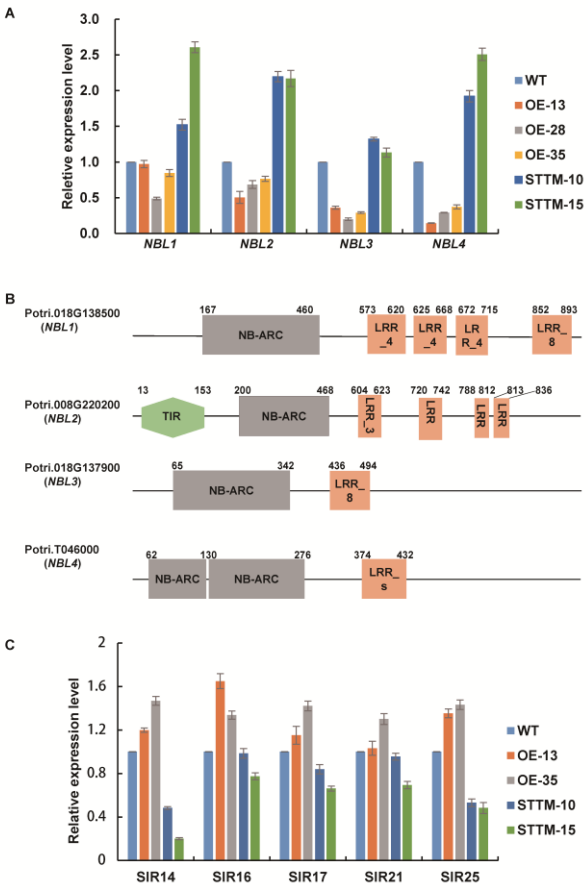

**Figure 4**

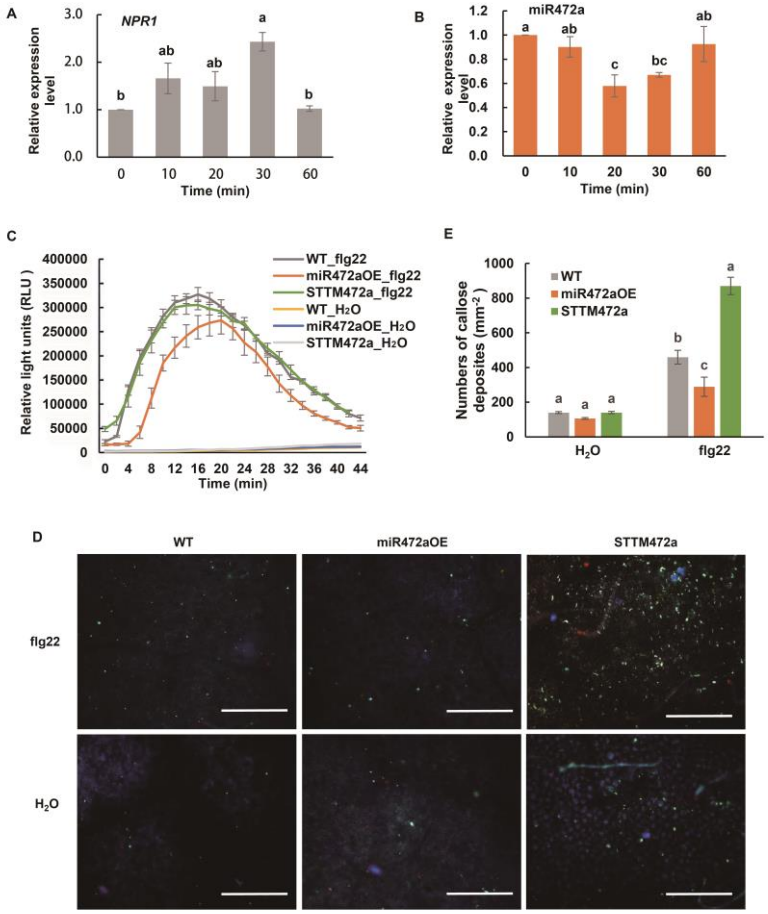

**Figure 5**

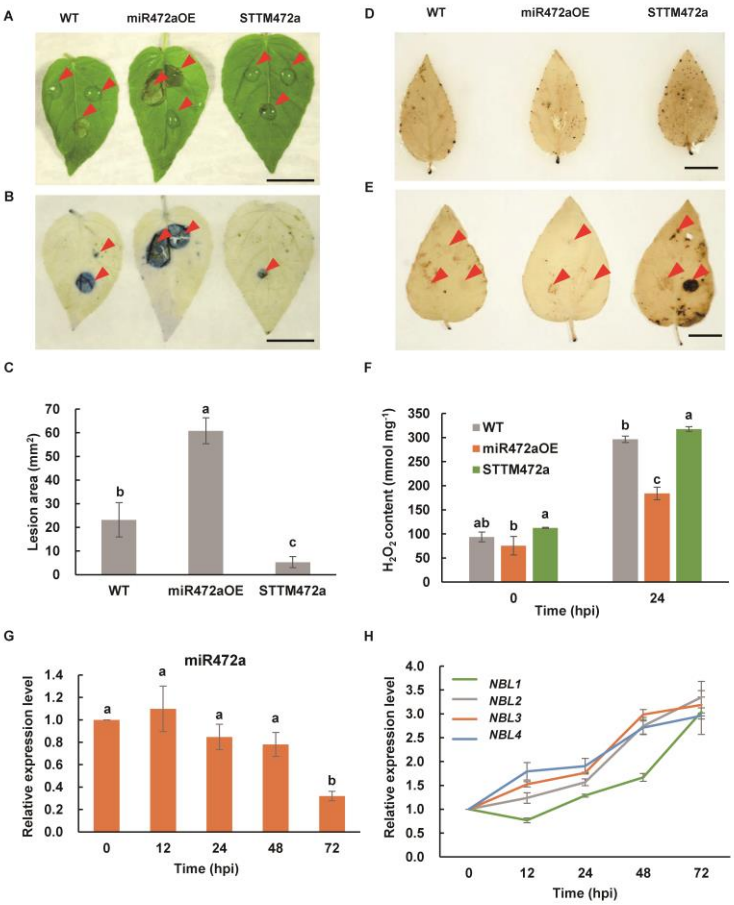

**Figure 6**

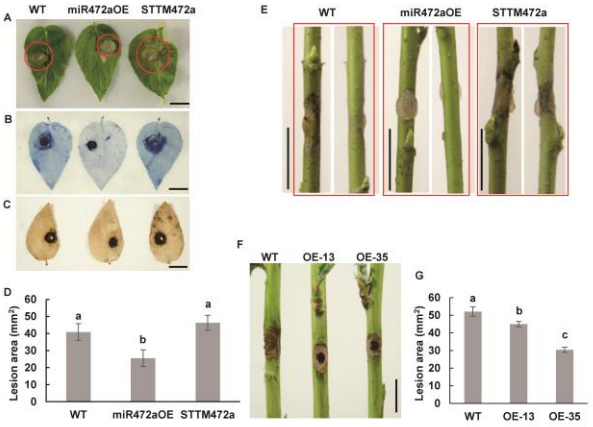

**Figure 7**

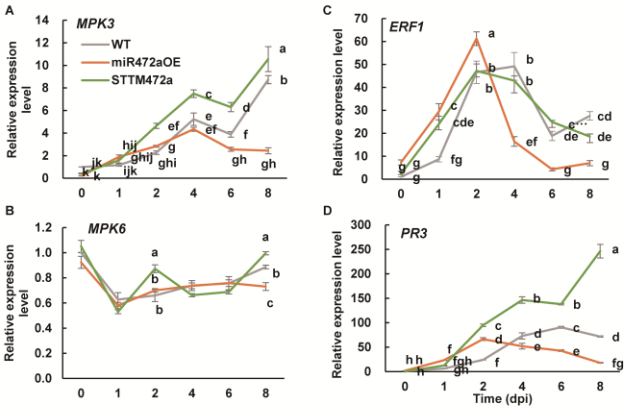

**Figure 8**